DOI: 10.1002/ange.201007031

Switchable Pores

Observation of Pore-Switching Behavior in Porous Layered Carbon through a Mesoscale Order–Disorder Transformation**

*Kasibhatta Kumara Ramanatha Datta, Dinesh Jagadeesan, Chidambar Kulkarni, Anushree Kamath, Ranjan Datta, and Muthusamy Eswaramoorthy**

Structural flexibility in biomacromolecules is a well-known phenomenon in nature.[1] For example, enzymes efficiently change their tertiary structures, the channels and cavities in which are reversibly modified to accommodate a guest molecule. The high specificity of enzymes in biologically important reactions is primarily attributed to their ability to change their structures in response to external stimuli. Taking a cue from nature, researchers are now looking for ways to make structurally flexible porous materials, as such materials could find wide-ranging application in catalysis, separation, sensors, fuel cells, and gas storage owing to their unique properties and functions.[2–4] Recently, metal–organic frameworks (MOFs) were shown to modify their framework structure in response to chemical or physical stimuli.[5,6] However, such a rearrangement of structure is not possible in rigid inorganic porous solids, such as zeolites, activated charcoal, and mesoporous silica.[5] Considering their industrial significance, structural flexibility in these porous materials would be very advantageous for the size-selective separation of molecules or switching between different properties of the material itself. Herein, we report the first observation of a reversible, mesoscale order–disorder transformation of a porous layered carbon (PLC) as a response to an applied mechanical force. The PLC containing crystallographically oriented graphene nanocrystallites on its layers was synthesized by graphitizing glucose within an aminoclay template. Although clay galleries have been used previously to make structurally rigid, porous carbon materials containing nanographene domains, these materials failed to show any mesoscale, long-range order replicating the stacked clay layer structure.[7,8] On the other hand, carbon materials obtained by using mesoporous silica as the template are often amorphous and exhibit ordered but rigid pores replicating the template.[9,10] In contrast to these rigid carbon materials, the PLC that we obtained showed a flexible pore size associated with a mesoscale order–disorder transformation, which we exploited for the size-selective separation (sorption) of dye molecules.

We used an aminoclay template to make layered carbon.[11,12] Aminoclay is an organophyllosilicate of approximate composition $R_8Si_8Mg_6O_{16}(OH)_4$ (in which $R = CH_2CH_2NH_2$) consisting of octahedrally coordinated MgO/OH sheets (brucite) overlaid on both sides with a tetrahedrally coordinated aminopropyl-functionalized silicate network.[11,12] Since the amine groups get protonated in water, the clay layers can readily be exfoliated owing to charge repulsion between the layers.[13,14] The exfoliated clay in water consists of a single layer or bundles containing a few layers (nanobundles). The dispersed layers can be restacked by the addition of ethanol (appearance of a white precipitate). In the present study, we first mixed a solution of glucose with a transparent aminoclay dispersion and then induced the stacking of clay layers/nanobundles by adding ethanol (see Scheme S1 in the Supporting Information). During the precipitation, glucose molecules get trapped in between the layers as well as in the space between the nanobundles. Thermogravimetric analysis (TGA) of the resulting composite after the excess glucose had been washed out with ethanol showed nearly 60% weight loss, mainly as a result of the removal of glucose (results not shown). Carbonization of the composite and subsequent etching of the clay, followed by filtration, left porous layered carbon (PLC). The absence of Si and Mg peaks in the energy-dispersive X-ray spectrum of the resulting PLC confirmed the complete removal of the clay template (see Figure S1 in the Supporting Information).

The powder X-ray diffraction pattern of the resulting PLC is shown in Figure 1a. The low-angle diffraction peak at $2\theta = 1.27°$ corresponding to a basal distance of 6 nm confirms the existence of mesostructural order in the carbon after the removal of the clay. Considering that the basal distance of the clay–glucose composite is 2.5 nm (and that this peak is lost on carbonization), it is unlikely that the individual clay layers would have acted as the template to generate this large d spacing of 6 nm. The PLC with a large d spacing (6 nm) therefore originates from the carbonization of glucose mostly trapped between the clay nanobundles, which are 2–3 layers thick, during the precipitation. The broad peak at $2\theta = 25°$ (the characteristic d_{002} graphitic peak in the higher-angle XRD pattern) indicates that the PLC is composed of nano-

[*] K. K. R. Datta, Dr. D. Jagadeesan,[+] C. Kulkarni, A. Kamath, Prof. M. Eswaramoorthy
Chemistry and Physics of Materials Unit and DST Unit on Nanoscience, Jawaharlal Nehru Centre for Advanced Scientific Research (JNCASR)
Jakkur P.O., Bangalore 560064 (India)
Fax: (+91) 80-2208-2766
E-mail: eswar@jncasr.ac.in
Homepage: http://www.jncasr.ac.in/eswar/
Dr. R. Datta, Prof. M. Eswaramoorthy
International Centre for Materials Science, JNCASR
Jakkur P.O., Bangalore 560064 (India)
[+] Present address: Lash Miller Chemical Laboratories
University of Toronto, Ontario M5S 3H6 (Canada)

[**] We thank Prof. C. N. R. Rao, FRS for his valuable suggestions and support throughout this project. K.K.R.D. thanks Dr. A. Gomathi and P. Kanoo for Raman and vapor-sorption measurements.
Supporting information for this article is available on the WWW under http://dx.doi.org/10.1002/anie.201007031.

© 2011 Wiley-VCH Verlag GmbH & Co. KGaA, Weinheim

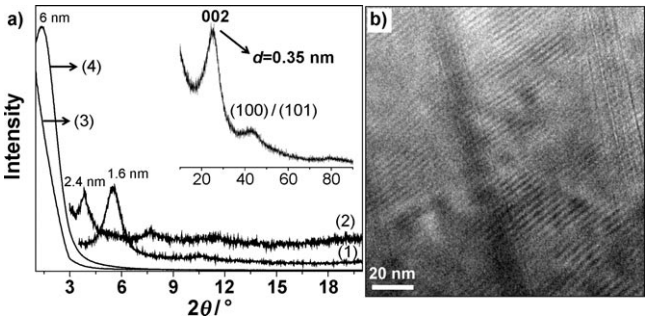

Figure 1. a) Low-angle XRD patterns of 1) the aminoclay, 2) the clay–glucose composite before carbonization, 3) the clay–glucose composite after carbonization, and 4) the clay–glucose composite after carbonization followed by etching of the clay to yield porous layered carbon (PLC). The wide-angle XRD pattern of PLC is shown in the inset. b) High-resolution TEM image of the porous layered carbon.

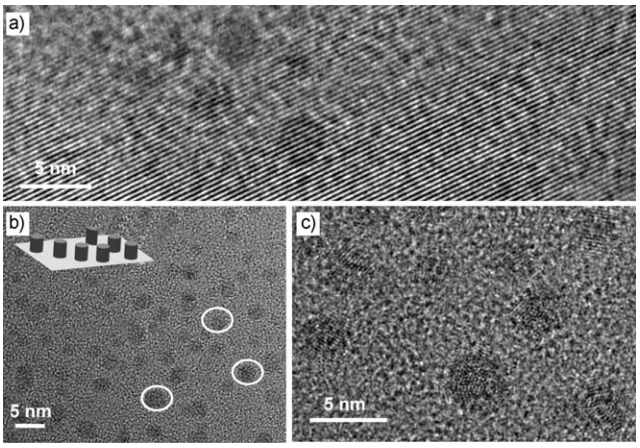

Figure 2. High-resolution TEM images of PLC showing pillarlike structures (highlighted by white circles). The inset in (b) shows a model of the pillars.

crystals of graphite. The crystallite width (perpendicular to the basal plane) calculated from the Scherrer formula is around 2.0 nm and is probably made up of 5–7 layers of graphene.[15]

A TEM image of the PLC sample obtained with an FEI TITAN^3 transmission electron microscope clearly shows the existence of a layered structure with a spacing between the layers of about 2.5 nm (Figure 1 b) and a wall thickness around 3 nm. Occasionally, we have also observed regions in which the wall thickness was in the range of 3–4 nm and the spacing between the layers varied between 2 and 4 nm. Such values are typical of a flexible layered structure (see Figure S2 in the Supporting Information). A low-magnification TEM image (top view) showed the porous nature of the layers composed of interconnected nanoparticles of 1–3 nm in size (see Figure S3 in the Supporting Information). The voids between the interconnected particles are well below 1.5 nm. Interestingly, the electron-diffraction pattern observed for this region showed single-crystalline behavior, which indicates a crystallographically well-oriented mesoscopic arrangement of the nanocrystallites. The high-resolution TEM image of a layered surface clearly confirms such an orientation, as the lattice fringes observed for the hexagonal carbon were continuous over a long distance (approximately 50 nm).[16–18] We found a significant number of dark contrast regions, each of which was about 3 nm in size, that probably originate from the pillarlike structures present between the layers (Figure 2). Most of these pillars are crystallographically oriented with the nanocrystals present in the layer. The PLC was found to be less stable under an electron beam, probably because of the presence of a large number of defects. This observation is also consistent with previously reported nanographenes, the instability of which is caused by the presence of pores that introduce defects along the edges.[19] Nevertheless, TGA showed that the thermal stability of the PLC is comparable to that of multiwalled carbon nanotubes (MWCNTs; Figure 3 a).[20]

Raman analysis of the PLC showed the appearance of an equally strong D band (at 1325 cm^{-1} for the defect sp^3-hybridized carbon atoms) in addition to the G band

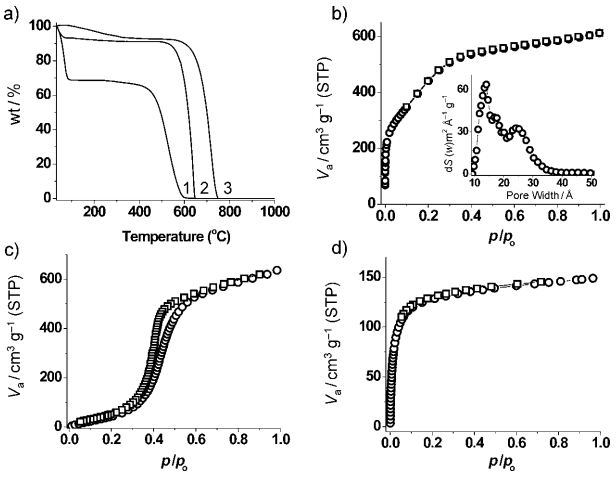

Figure 3. a) TGA curves for 1) PLC, 2) MWCNTs, and 3) graphite in the presence of O_2 gas. b) N_2 adsorption (circles)–desorption (squares) isotherm at 77 K for PLC; the inset shows the corresponding pore-size distribution; d$S(w)$ is the differential surface area. c) Vapor-sorption isotherm (adsorption: circles, desorption: squares) of H_2O over PLC at 298 K. d) Vapor-sorption isotherm (adsorption: circles, desorption: squares) of C_6H_6 over PLC at 298 K. STP = standard temperature and pressure.

(1590 cm^{-1}). The appearance of this D band is quite understandable, as defects of this type are commonly associated with such porous structures made of nanocrystallites (see Figure S4 in the Supporting Information).[21,22]

The nitrogen adsorption–desorption isotherms obtained for the PLC at the temperature of liquid nitrogen (77 K) show mostly type I behavior, with a two-step rise in adsorption at low p/p_0 values without hysteresis (Figure 3 b). Indeed, type I and type II isotherms for spherical or platelike particles usually will not show any hysteresis. The initial steep rise in the adsorption isotherm at very low p/p_0 values (less than 0.1) can be accounted for by the existence of micropores originating from within the layers (as the layers are composed of interconnected nanoparticles). The second rise in the adsorption is in the p/p_0 range 0.1–0.4, bordering the

 © 2011 Wiley-VCH Verlag GmbH & Co. KGaA, Weinheim

mesopore region, but is not prominent like that observed for MCM-type materials. It may be associated with capillary condensation between the platelike layered structures.[23] The nonlocal density functional theory (NLDFT) method was used to calculate the pore size and showed two types of pores: one with a width of 1.4 nm in the micropore region and the other with a width of 2.4 nm in the mesopore region (inset in Figure 3b). The specific surface area calculated by Brunauer–Emmett–Teller (BET) theory is about 1628 $m^2 g^{-1}$. However, caution must be exercised when measuring the surface area of materials containing micropore regions.[24]

Vapor-sorption experiments showed no significant uptake of water in the region corresponding to lower p/p_0 values but showed a steep rise in adsorption as the pressure increased ($p/p_0 \approx 0.4$; Figure 3c). On the other hand, benzene adsorption shows type I behavior, with strong uptake at very low p/p_0 values (Figure 3d). This variation in the adsorption behavior for water and benzene indicates that the PLC, because of its graphitic structure, can interact well with nonpolar molecules, such as benzene. It can also interact with polar molecules owing to the presence of the oxygen-containing edges of the nanocrystallites. Indeed, elemental analysis of the PLC showed nearly 15% oxygen and 5% nitrogen in addition to carbon (see Figure S5 and Table S1 in the Supporting Information). The IR spectrum also showed bands corresponding to N–H, C–O, C=C, and O–H stretching (see Figure S5b).

Interestingly, when the PLC was dispersed in water and then centrifuged, the mesoscale order was lost, as seen from the absence of a low-angle peak in the XRD pattern (Figure 4a). The N_2 adsorption–desorption isotherm clearly displayed type I behavior for this sample with a BET specific surface area of 1543 $m^2 g^{-1}$ (Figure 4c; see also Table S2 in the Supporting Information). A pore size of around 1.4 nm was calculated by the NLDFT method, which did not show the existence of any mesopores, perhaps as a result of a collapse of the space between the layers upon centrifugation. The centrifugal (shear) force required to cause this collapse was found to be 17 N for 1 gram of sample. However, we did not observe any control in the degree of buckling by reducing the centrifugal (shear) force below 17 N. Since the micropores are mainly derived from the interconnected crystallites within the layer, there was no appreciable variation. To our surprise, the mesoscale order was regained when the sample was again dispersed in water and was then allowed to settle on its own or was separated by filtration (Figures 4b and 5).

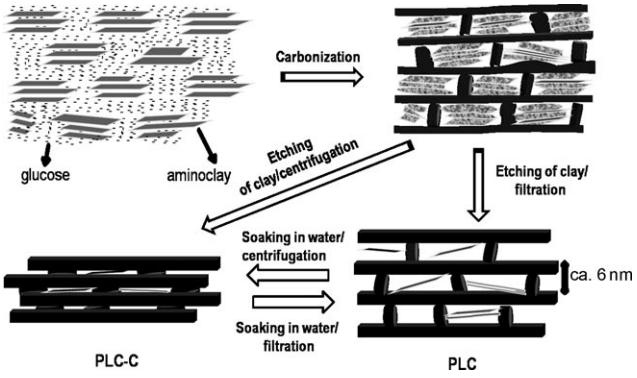

Figure 5. Stepwise formation of ordered and disordered layered flexible carbon materials.

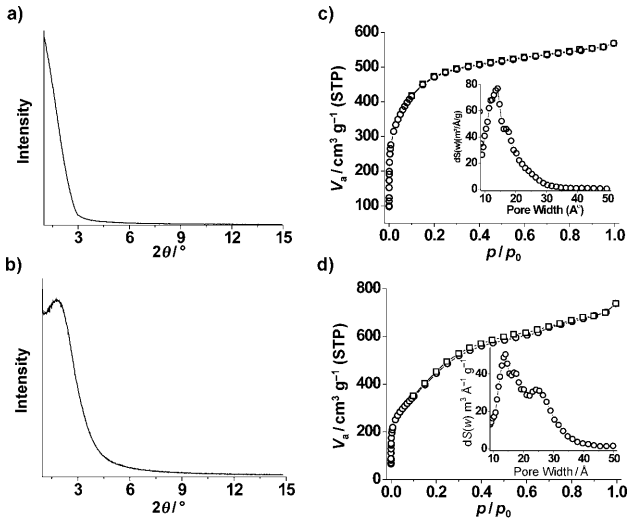

Figure 4. Low-angle XRD patterns showing the reversible nature of porous layered carbon: a) after soaking of PLC in water, followed by centrifugation (PLC-C), b) after soaking of the sample in (a) in water, followed by filtration. c,d) N_2 adsorption (circles)–desorption (squares) isotherms at 77 K corresponding to (a) and (b), respectively; insets show the pore-size distribution.

In agreement with the reversible change in structure, the adsorption behavior also reappeared with the return of two types of pore size (Figure 4d). Although there is a slight variation in the isotherms of the original sample and the sample recovered after soaking in water and filtration, as the structure of PLC is not as rigid as that of zeolites, the appearance and disappearance of the mesopore region as a result of the order–disorder transformation is clear. This process was reversible and reproducible (see Figure S6). Indeed, when the porous layered carbon was synthesized by etching of the clay followed by centrifugation (PLC-C; rather than filtration), the mesoscale order was not observed (see Figure S6a). The adsorption isotherm of this material exhibited type I behavior, and a pore size around 1.4 nm was found (see Figure S6d). However, when the same sample was dispersed in water and was then allowed to settle or was filtered, the resulting product showed the mesoscale order in the low-angle XRD pattern, and the associated isotherm indicated the presence of two types of pores: one with a width of about 1.4 nm and the other with a width of about 2.5 nm (see Figure S6b,e). Dispersion of the sample again in water followed by centrifugation led to the disappearance of the mesoscale order as well as the mesopores (see Figure S6c,f).

The structural reversibility of PLC between mesoscale order and disorder, as induced by filtration and centrifugation, clearly shows the existence of flexibility in the layered stacking. Such an arrangement can be envisaged if the carbon interlayers are loosely held by the pillarlike structure. The formation of such pillars is possible in our case, since the

 © 2011 Wiley-VCH Verlag GmbH & Co. KGaA, Weinheim

glucose molecules trapped in the space (in the stacking direction) between the clay nanobundles during precipitation could provide pillarlike carbon structures on carbonization that could keep the carbon layers from collapsing (Figure 5). The exact nature of the chemical bonding connecting the pillars with the carbon layers is difficult to ascertain. However, we believe that the oxygen- and nitrogen-containing functional groups play an important role in the loose connection of the pillarlike structures with the layers. The absence of pore-switching behavior on removal of the functional groups by high-temperature heat treatment (above 700 °C in an N_2 atmosphere or above 400 °C for 6 h in H_2) signifies the importance of the functional groups for pore switching. When there is no centrifugal force and the PLC is allowed to settle on its own in water, the layers may have a breathing space between them supported by the pillars and the water molecules in between. Similarly, when the PLC-C sample is soaked in water, the buckled, pillarlike carbon structures revert back to their original shape. Although the presence of nanosheets between the layers cannot be ruled out, their contribution to the order–disorder transformation by exfoliation/stacking is unlikely, as we observed collapse of the order only on the application of a centrifugal force. TGA measurements showed that PLC holds about 10 wt% more water than PLC-C (weight loss below 150 °C; see Figure S7), which suggests that the interaction of water is essential for reorientation of the pillar structures. However, when a centrifugal force (or shear force) is applied, the layers slide over one another through buckling of the pillars; this action could squeeze out the water from between the layers.

The variation in pore size as a result of structural changes was demonstrated by the selective sorption of dye molecules of different molecular sizes (Congo red, alizarin yellow). The molecular sizes of Congo red and alizarin yellow were calculated to be 2.6 and 1.3 nm, respectively (see computational details in the Supporting Information). As-prepared PLC, centrifuged PLC (PLC-C), and an activated charcoal (AC) were compared in the dye-sorption studies. The samples were soaked in the dye solution for a period of 12 h, and the extent of sorption was determined from the intensity of the absorption maxima of the remaining dye in the supernatant (see the Experimental Section and Figure S8).

A strong decrease in the absorption intensity of the Congo red solution was observed for PLC and not for the PLC-C and AC samples. This result clearly supports the presence of large pores (2.5 nm), which help to maximize the sorption of Congo red, in PLC. Since PLC-C and AC contain pores (only micropores) that are smaller than the size of Congo red, they show poor sorption. On the other hand, with alizarin yellow (1.3 nm), which is about half the size of a Congo red molecule, almost equal sorption (strong reduction in the absorption intensity at 353 nm) was observed for all three samples. Furthermore, the sorption behavior of PLC and PLC-C in a mixed-dye solution was investigated by soaking each sample in a solution containing both Congo red and alizarin yellow. As expected, Congo red (absorbance at 499 nm) was sorbed selectively over PLC, whereas no sorption was observed for PLC-C. Reasonable sorption was detected for the smaller alizarin yellow molecule (absorbance at 350 nm) by both PLC and PLC-C, although PLC showed higher sorption of this smaller dye (see Figure S9).

In conclusion, we have described a new synthetic route to porous layered carbon (PLC) composed of nanographenes. In this approach, aminoclay was used as a template. The carbonization of glucose within the aminoclay template left pillared carbon with a flexible framework, the mesostructured periodicity of which could be induced to undergo dynamic alteration. The pore-switching behavior of the PLC upon exposure to a mechanical force (centrifugal force) was demonstrated by the size-selective sorption of dye molecules. We further envisage the possible use of these dynamic pores for the selective screening of smaller biomolecules, dyes, toxic gases, and other molecules.

Experimental Section

The aminoclay was prepared by a previously reported method.[13] In a typical synthesis, 3-aminopropyltriethoxysilane (1.3 mL, 5.85 mmol) was added dropwise to an ethanolic solution of magnesium chloride (0.84 g, 3.62 mmol) at room temperature. The white slurry obtained after 5 min was stirred overnight, and the precipitate was isolated by centrifugation, washed with ethanol (50 mL), and dried at 40 °C.

The aminoclay (1 g) was exfoliated in water (10 mL), and glucose (3 g) was added to it. The resulting solution was aged for 12 h, and then ethanol was added to cause precipitation. The precipitate that formed was dried at 50 °C. The resulting brown powder (the clay–glucose composite) was placed in a clean silica boat and then carbonized at 600 °C in an N_2 atmosphere for 6 h with a heating rate of 5 °C min^{-1}. The black carbonized products were demineralized with 12% HCl and 13% HF for 12 h to remove all of the clay structure as the respective salts. Layered porous carbon materials obtained by centrifugation (6000 rpm) are referred to as PLC-C, whereas filtered samples are referred to as PLC. The centrifugal (shear) force was calculated by using the expression $M\omega^2 R$, in which M is the mass of the sample, ω is the angular velocity, and R is the rotation radius. The porous carbon materials were obtained as black powders (see Scheme S1 in the Supporting Information).

Dye sorption: A stock solution of the dye (1.2 g L^{-1}) was prepared by dissolving the dye (Congo red or alizarin yellow) in water (10 mL). In each experiment, the porous adsorbent (10 mg; PLC, PLC-C, or AC) was suspended in 2 g of the stock solution. Similarly, for selective dye sorption, equal volumes of the stock solutions (1.2 g L^{-1}) of Congo red and alizarin yellow were mixed, and PLC or PLC-C (10 mg) was added to this mixture. These solutions were allowed to stand for 12 h at 298 K to enable equilibrium to be reached. After ageing of the solutions, they were centrifuged to avoid potential interference from suspended scattering particles, and the residual dye concentration in the supernatant was measured with a UV/Vis spectrophotometer.

Received: November 9, 2010
Revised: January 10, 2011
Published online: March 29, 2011

Keywords: dye sorption · mesoporous materials · nanographene · nanostructures · pore switching

[1] D. L. Nelson, M. M. Cox, *Lehninger Principles of Biochemistry*, Macmillan, New York, **2000**, chap. 6.
[2] a) J. Rabone, Y.-F. Yue, S. Y. Chong, K. C. Stylianou, J. Bacsa, D. Bradshaw, G. R. Darling, N. G. Berry, Y. Z. Khimyak, A. Y. Ganin, P. Wiper, J. B. Claridge, M. J. Rosseinsky, *Science* **2010**,

 © 2011 Wiley-VCH Verlag GmbH & Co. KGaA, Weinheim

329, 1053; b) A. Ziv, A. Grego, S. Kopilevich, L. Zeiri, P. Miro, C. Bo, A. Müller, I. A. Weinstock, *J. Am. Chem. Soc.* **2009**, *131*, 6380.
[3] C. Serre, C. Mellot-Draznieks, S. Surblé, N. Audebrand, Y. Filinchuk, G. Férey, *Science* **2007**, *315*, 1828.
[4] Y.-J. Zhang, T. Liu, S. Kanegawa, O. Sato, *J. Am. Chem. Soc.* **2010**, *132*, 912.
[5] S. Horike, S. Shimomura, S. Kitagawa, *Nat. Chem.* **2009**, *1*, 695.
[6] S. Bureekaew, S. Shimomura, S. Kitagawa, *Sci. Technol. Adv. Mater.* **2008**, *9*, 014108.
[7] A. Bakandritsos, T. Steriotis, D. Petridis, *Chem. Mater.* **2004**, *16*, 1551, and references therein.
[8] Y. Xia, Z. Yang, R. Mokaya, *Nanoscale* **2010**, *2*, 639.
[9] R. Ryoo, S. H. Joo, S. Jun, *J. Phys. Chem. B* **1999**, *103*, 7743.
[10] S. Jun, S. H. Joo, R. Ryoo, M. Kruk, M. Jaroniec, Z. Liu, T. Ohsuna, O. Terasaki, *J. Am. Chem. Soc.* **2000**, *122*, 10712.
[11] S. L. Burkett, A. Press, S. Mann, *Chem. Mater.* **1997**, *9*, 1071.
[12] N. T. Whilton, S. L. Burkett, S. Mann, *J. Mater. Chem.* **1998**, *8*, 1927.
[13] A. J. Patil, E. Muthusamy, S. Mann, *Angew. Chem.* **2004**, *116*, 5036; *Angew. Chem. Int. Ed.* **2004**, *43*, 4928.
[14] K. K. R. Datta, C. Kulkarni, M. Eswaramoorthy, *Chem. Commun.* **2010**, *46*, 616.
[15] C. N. R. Rao, K. Biswas, K. S. Subrahmanyam, A. Govindaraj, *J. Mater. Chem.* **2009**, *19*, 2457.
[16] A. C. Ferrari, J. C. Meyer, V. Scardaci, C. Casiraghi, M. Lazzeri, F. Mauri, S. Piscanec, D. Jiang, K. S. Novoselov, S. Roth, A. K. Geim, *Phys. Rev. Lett.* **2006**, *97*, 187401.
[17] A. Dato, V. Radmilovic, Z. Lee, J. Phillips, M. Frenklach, *Nano Lett.* **2008**, *8*, 2012.
[18] J. Campos-Delgado, J. M. Romo-Herrera, X. Jia, D. A. Cullen, H. Muramatsu, Y. A. Kim, T. Hayashi, Z. Ren, D. J. Smith, Y. Okuno, T. Ohba, H. Kanoh, K. Kaneko, M. Endo, H. Terrones, M. S. Dresselhaus, M. Terrones, *Nano Lett.* **2008**, *8*, 2773.
[19] D. Teweldebrhan, A. A. Balandin, *Appl. Phys. Lett.* **2009**, *94*, 013101.
[20] D. Bom, R. Andrews, D. Jacques, J. Anthony, B. Chen, M. S. Meier, J. P. Selegue, *Nano Lett.* **2002**, *2*, 615.
[21] A. C. Ferrari, *Solid State Commun.* **2007**, *143*, 47.
[22] a) M. S. Dresselhaus, A. Jorio, M. Hofmann, G. Dresselhaus, R. Saito, *Nano Lett.* **2010**, *10*, 751; b) T. Enoki, K. Takai, V. Osipov, M. Baidakova, A. Vul, *Chem. Asian J.* **2009**, *4*, 796.
[23] J. C. Groen, L. A. A. Peffer, J. Pérez-Ramírez, *Microporous Mesoporous Mater.* **2003**, *60*, 1.
[24] K. Matsuoka, Y. Yamagishi, T. Yamazaki, N. Setoyama, A. Tomita, T. Kyotani, *Carbon* **2005**, *43*, 876.

 © 2011 Wiley-VCH Verlag GmbH & Co. KGaA, Weinheim